

VIBRO-ACOUSTICS OF THE SOUTH INDIAN DRUM: MRIDANGAM

G. Sooraj

*Indian Institute of Technology Madras
Chennai 600036 India
email: me15s052@smail.iitm.ac.in*

Chandramouli Padmanabhan

*Indian Institute of Technology Madras
Chennai 600036 India
email: mouli@iitm.ac.in*

This paper presents a summary of the ongoing research to develop a vibro-acoustic model of Mridangam - A South Indian drum. Various components of this instrument such as the wooden body structure, acoustic cavity inside the body as well as the membranes of the drum are analyzed to understand their role in producing the music. The analysis involves both experiments and finite element simulations. The coupled behaviour of the membrane and air cavity is demonstrated using an idealised mridangam membrane model from the literature.

Keywords: Mridangam shell modal analysis, Acoustics of shell cavity, Coupled-vibroacoustics

1. Introduction

Natya Shaastra (200 BCE - 200 CE), one of the oldest systems of music classification, recognizes four basic categories of musical instruments based on the vibration characteristics [1]. Both Johannes de Muris and Victor Charles Mahillon have adapted this classification from Natya Shaastra to Western music [2, 3].

Mridangam, classified as a membranophone, has a double cone barrel shaped wooden cavity and membranes on its ends. Sir C V Raman [4] was the first to investigate its vibro-acoustics and found out experimentally that the central black spot makes the first nine modes to be harmonic multiples. Ramakrishna and Sondhi [5] arrived at an optimum density ratio and diameter of the black patch, which can generate integer multiples of the fundamental natural frequency. A detailed experimental and computational study of the mridangam has however not been carried out to date.

2. Studies on Hollow Wooden Body

The hollow wooden body is the heaviest component of a Mridangam. The most important feature in its construction is the shape of the cavity. At the ends, they are cylindrical. Further inside it becomes a barrel shape with maximum diameter slightly offset from the mid-span of the body. Thus the thickness varies at each cross section. Most commonly used wood is Jack-fruit tree wood, which is abundant in South Asia. The making of the specimen involves cutting of the log to the approximate length of the Mridangam, chipping it to an approximate conical shape using an axe, fine turning the outside and finally boring the inside. The profile of the 24 inch mridangam body used for the study was measured and is shown in Fig. 1.

2.1 Modal Analysis Experiment

The specimen was subjected to modal analysis experiment under a free-free boundary condition simulated by suspending it using bungee cord with a soft spring, as shown in Fig. 2. Roving hammer impact testing was carried out to extract the frequency response functions (FRFs). For a clear understanding of the mode shapes, 128 nodes were selected for analysis - 16 azimuthal points each on 8 circles along the axis of the barrel.

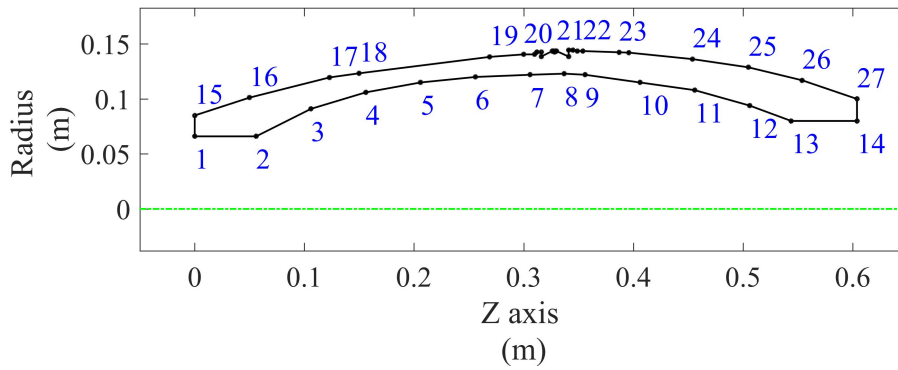


Figure 1: Measured 2D Profile



Figure 2: Experimental Setup - Mridangam Body Modal Analysis

Fig. 3 shows three typical accelerance FRFs measured on the mridangam wooden body. Clearly defined peaks are observed at 487 Hz, 646 Hz, 1055 Hz, 1184 Hz and 1410 Hz. A discussion on the mode shapes with their comparison with simulation is provided later.

2.2 Finite Element Analysis

To begin with a simple model with a smooth outer profile was generated. In the next step, a more detailed model accounting for the outer grooves near the centre was generated. Average density of the wood was obtained by first weighing the annular body and then dividing by the volume calculated from the CAE model. The CAE model was generated from the measurement of the profile as shown in Fig. 1. The material was assumed to be isotropic initially with a Young's Modulus of 10 GPa

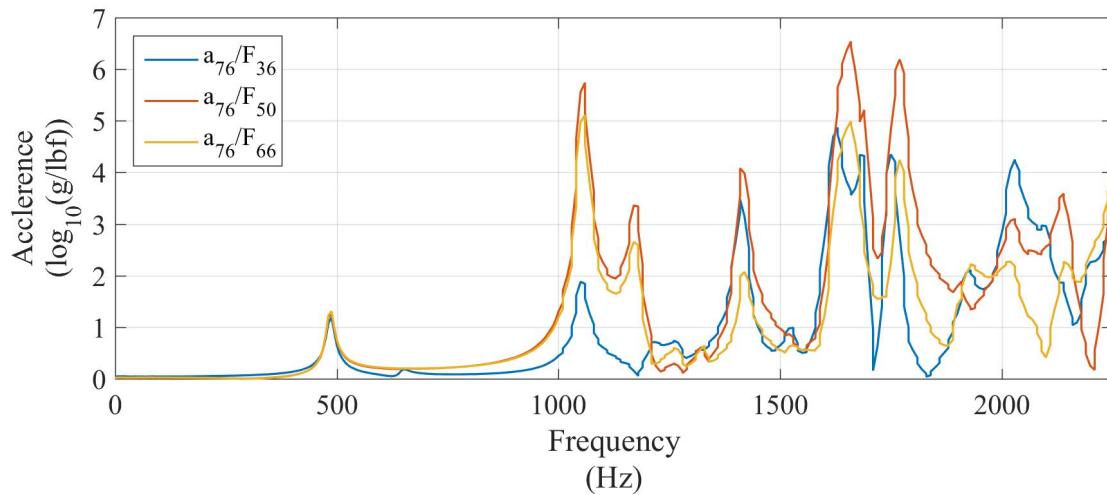


Figure 3: Typical FRFs of wooden body vibration

obtained from the literature. All the finite element analyses were carried out in Simulia ABAQUS [6]. A mesh convergence study was carried out on all these FE models to ensure that the errors for the first 15 modes are acceptable.

2.3 Results and Discussion

The first natural frequency predicted from FE model was 1115 Hz, which was much higher than what was observed from the experiments. The following values were 1548 Hz, 1989 Hz, 2072 Hz and 2137 Hz. The first and fifth mode shapes are shown in Figs. 4-5, with the fifth representing a bending mode; these are for the solid element based model. With shell elements the natural frequencies were fairly close (within 4-5%) to the solid element results.

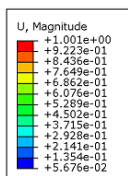


Figure 4: First mode shape (1115 Hz)

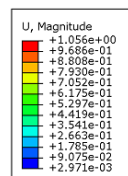


Figure 5: Fifth mode shape(2137 Hz)

The frequencies measured from experiment are considerably different from the simulation values. However, it was noticed that the ratio of the natural frequencies with respect to the fundamental frequency were comparable for the first 3-4 modes. When the Young's modulus was changed in the FE model to 3 GPa, it was found that the experimental and simulation results were quite close. To verify the modulus of elasticity, a wooden specimen was tested on a UTM for its stress-strain relation in the linear range. These tests indicated that the assumption was a reasonable one. As evident from the Figs. 6-8, the lower modes have a very good agreement with the CAE modes. The modal assurance criterion (MAC values) between experimental and FE modeshapes are almost 0.8 till the 4th mode. Hence, one can see that the isotropic assumption is reasonable. The ratios from simulation do not match well with those from experiment for the 4th/5th modes. This is probably due to the

Table 1: Natural Frequency Comparison for the Wooden body structure

| Mode | NF | | | NF Ratio | | |
|------|------|---------|---------|----------|---------|---------|
| | Exp | FEM- Sd | FEM- Sh | Exp | FEM- Sd | FEM- Sh |
| 1 | 487 | 1115 | 1052 | - | - | - |
| 2 | 646 | 1548 | 1433 | 1.33 | 1.39 | 1.36 |
| 3 | 1055 | 1989 | 1996 | 2.16 | 1.78 | 1.90 |
| 4 | 1184 | 2072 | 2105 | 2.43 | 1.86 | 2.00 |
| 5 | 1410 | 2137 | 2164 | 2.89 | 1.92 | 2.06 |

NF: Natural Frequency, Exp: Experimental, Sd : Solid Element, Sh : Shell Element

material variations seen in the sample used for the experiment.

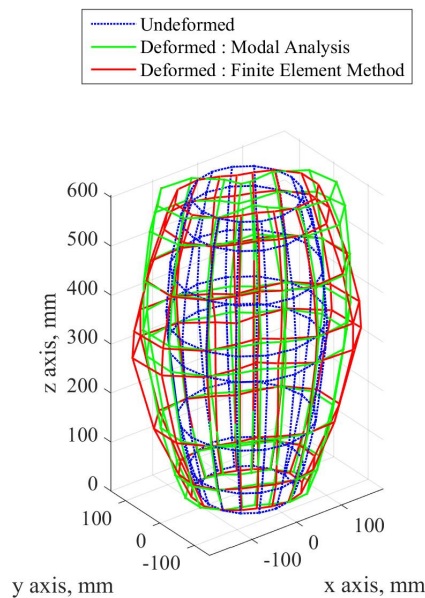


Figure 6: Mode 1

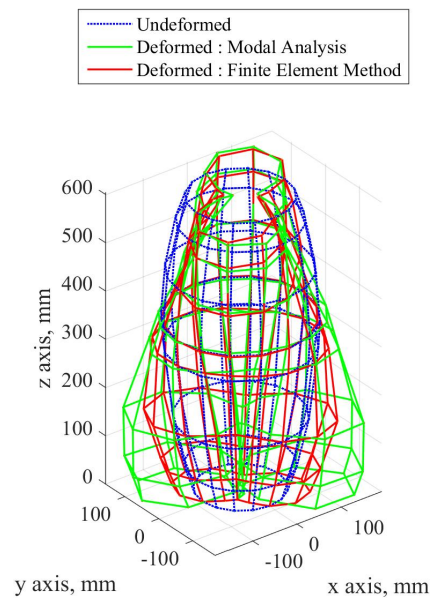


Figure 7: Mode 2

3. Studies on Air Cavity

The air cavity inside the wooden body couples the two membranes on either side. It also has the potential to selectively sustain certain modes of the membranes, and thus affect the overall sound of the instrument. It is crucial to identify the effect of the cavity in the coupled system, and thus a stand-alone study is carried out first.

3.1 Cavity Acoustics Experiment

The openings on the wooden body were closed using plexiglass plates as shown in Fig. 10. These were firmly attached to the wooden rim using the same arrangement which that keeps the leather braided membranes in place. The small end was fixed with a 30 W speaker which is the exciter and other end had an arrangement to traverse a microphone into the cavity to take the response measurement. The test signals used were white noise (from 0-3200 Hz) and also swept sine, which were generated from a Dactron 4-channel data acquisition system. An intermediate amplifier was used for the excitation signal.

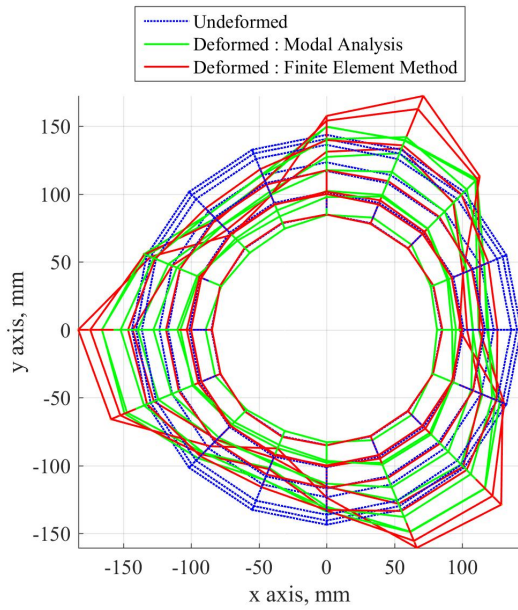


Figure 8: Mode 3

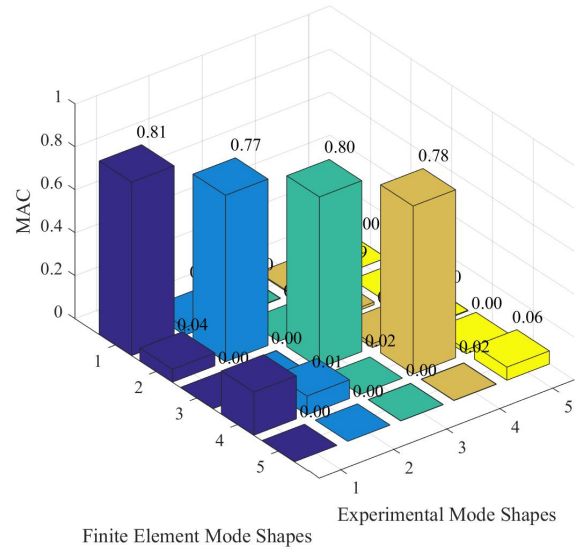


Figure 9: Modal Assurance Criterion



Figure 10: Experimental Setup : Wooden Shell Cavity
Inset : Microphone and Speaker

The primary focus was to extract the natural frequencies of the air cavity. Fig. 11 shows the autospectrum of the microphone signal for a swept sine excitation from 100 Hz to 2000 Hz over a span of 200 seconds. Clearly defined peaks were observed at 370 Hz, 628 Hz, 893 Hz, 1152 Hz and 1420 Hz. The peak at around 140 Hz (marked with red circle) was found to be related to the support vibration, as changing the support structure changed both the frequency and amplitude of the response. Further investigation is needed to understand this effect.

3.2 Finite Element Analysis

A FEA was carried out in Abaqus, with AC3D8 elements for modelling the cavity. For the cavity both density of air and bulk modulus were provided as inputs. Again, a convergence study was done to ensure that the first 10 modes were fairly accurate. The corresponding mode shapes were also obtained. The first 3 modes are axial modes (Fig. 12, RED - Positive Pressure, BLUE- Negative Pressure) and first non axial mode is at 896 Hz. Next axial mode is observed at 1113 Hz, followed by an array of non-axial modes. A qualitative classification of these modes is presented in Table 2.

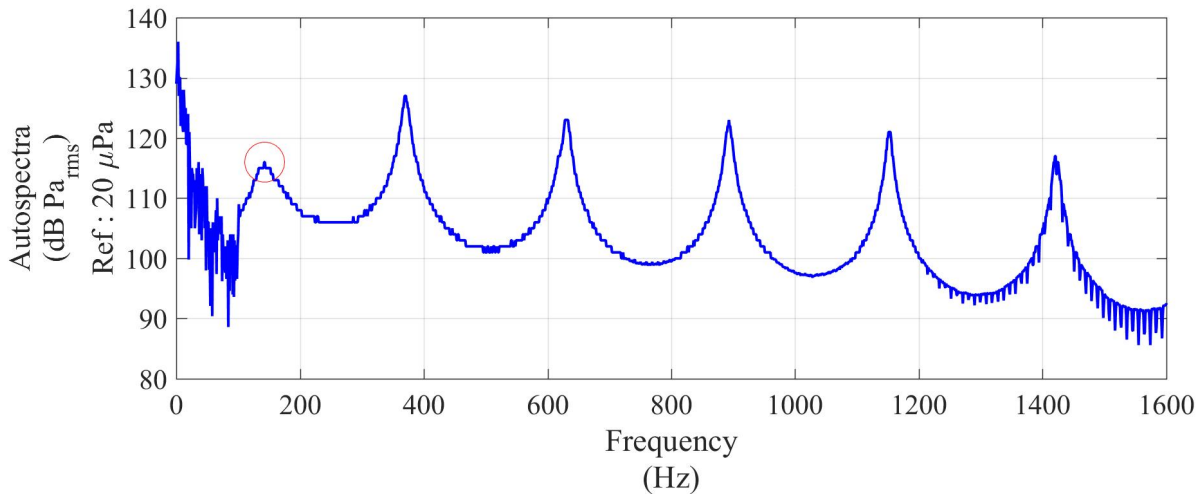


Figure 11: Autospectra of acoustic response

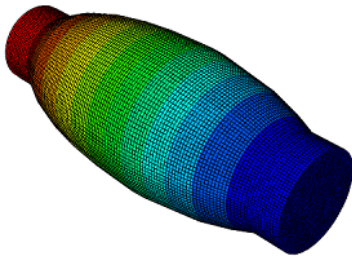


Figure 12: Aircavity Mode 1 (370 Hz)

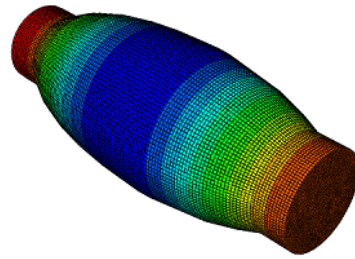


Figure 13: Aircavity Mode 2 (628 Hz)

3.3 Discussion of the results

The first two modes from the simulation match well with the experimental data. Certain modes were not visible in the experimental results (refer Table 2).

Table 2: Natural Frequency Comparison : Aircavity

| Mode | FEA | | Experimental Natural Frequency (Hz) | Error |
|------|------------------------|------------|--|-------|
| | Natural Frequency (Hz) | Nature | | |
| 1 | 361 | Axial | 370 | 2.55 |
| 2 | 611 | Axial | 628 | 2.72 |
| 3 | 857 | Axial | | - |
| 4 | 896 | Transverse | 893 | |
| 5 | 1092 | Transverse | - | - |
| 6 | 1113 | Axial | 1152 | - |
| 7 | 1280 | Transverse | 1420 | 9.86 |

It is expected that only the first few modes of the cavity will participate strongly in the vibro-acoustics and the current FE model predicts those modes quite well. Next a coupled cavity-membrane model is considered.

4. Simulation of a Coupled System of membranes and air cavity

The membranes are the vital part of a mridangam. At this point the information about the real membrane used is somewhat uncertain. There is a centrally loaded primary membrane on the small side and uniform secondary membrane on the other. The primary membrane is simulated using the data from Ramakrishna and Sondhi [5], which ensures that the natural frequencies are approximately harmonic. The secondary membrane uses the same property of the unloaded part of the primary membrane. Primary membrane has an outer radius of 65 mm and black spot of radius 26 mm. The density with black spot is 7812.5 kg/m^3 and without black spot is 800 kg/m^3 . The outer radius of secondary membrane is 100 mm. In built capabilities of Abaqus to model structural acoustics coupling were exploited by judicious use of TIE constraints.

4.1 Results and Discussion

The primary interest is in comparing the coupled system frequencies with the individual component frequencies. Table 3 lists the uncoupled membrane and cavity frequencies along with the coupled

Table 3: Natural Frequency Comparison: Coupled System

| Aircavity | Pr. Membrane | Sc. Membrane | Coupled Sys. |
|-----------|--------------|--------------|--------------|
| | 102 (As) | | 99 (A) |
| | | 166 (As) | 154 (A) |
| | 195 | | 193 |
| | | 265 | 242 |
| | 296 | 355 | |
| | 302 (As) | | 287 (A) |
| 361 (Ax) | | | 294 |
| | | | 335 |
| | | 382 (As) | 343 (A) |
| | 397 | 442 | |
| | | | 391(A) |
| | | 525 | |
| 611 (Ax) | 484 (As) | | 481 (A) |
| 856 (Ax) | | | |

(Ax) - Axial Modes, (As) - Axisymmetric Modes, (A) - Axially Coupled Modes

membrane cavity frequencies. It is seen from Fig. 14 that the axisymmetric modes couple with the cavity quite well. However, a non-axisymmetric membrane mode (with nodal diameter) does not excite the cavity (Fig. 15). The second and third axisymmetric modes of the membranes are observed to couple with the first mode of the cavity. This can be attributed to the closeness in their frequency. The second cavity mode is only the twenty- fifth mode of the coupled system. Another important observation is that, the natural frequency ratios are altered by the coupling to the cavity. Hence, to have a harmonic relation in the coupled system, the uncoupled membrane natural frequencies should not be exactly harmonic but only nearly so.

5. Conclusion

The work presented in this paper is the efforts towards building a vibro acoustic model of a Mridangam, which can be further used to carry out simulations on sound radiation. The components of

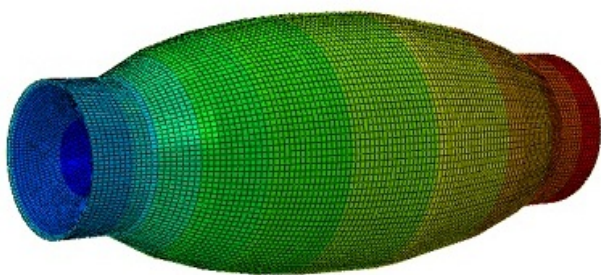


Figure 14: Axisymmetric membrane mode coupling with the cavity

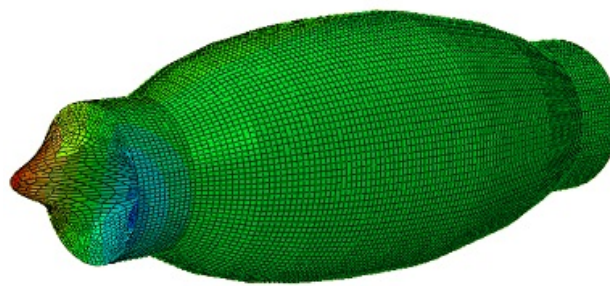


Figure 15: Non- axisymmetric membrane mode with weak cavity coupling

Mridangam : wooden body and air cavity were studied using experiments and Finite Element models. Preliminary study of the coupled system with a theoretical membrane was also carried out. Further steps include detailed study and modelling of the membranes and their integration to the system.

REFERENCES

1. Swatantra Sharma, *Fundamentals of Indian Music*, Pratibha Prakashan, Delhi(1996).
2. P. Jeserich, *Musica Naturalis: Speculative Music Theory and Poetics, from Saint Augustine to the late Middle ages in France*, Translated by M J Curley and S Rendall, Johns Hopkins University Press, Baltimore, p-239 (2013).
3. V. C. Mahillon, *Eléments d'acoustique musicale & instrumentale*, Mahillon, France (1874).
4. C. V. Raman, The Indian Musical Drums, *Proceedings of the Indian Academy Of Science A1*, 179-188 (1935)
5. B. S. Ramakrishna and M. M. Sondhi, Vibration of Indian Musical Drums regarded as composite membranes, *The Journal of the Acoustical Society of America*, Volume 26, Number 4 July, 523-529 (1954)
6. *Simulia Abaqus 6.12 User Manual*. [Online.] available: <http://abaqus.software.polimi.it/v6.12/index.html>.